ACCOUNTS of chemical research

pubs.acs.org/accounts Article

Deciphering the Local Environment of Single-Atom Catalysts with X-ray Absorption Spectroscopy

Yuanyuan Li and Anatoly I. Frenkel*

Cite This: *Acc. Chem. Res.* 2021, 54, 2660−2669 Read Online

ACCESS | Metrics & More | Article Recommendations

CONSPECTUS: To improve the reactivity of catalysts, two goals that are perhaps the most obvious but at the same time the most elusive ones are (1) to increase the number of active sites and/or (2) to enhance the intrinsic activity of each active site. Both seem realizable in single-atom catalysts (SACs), in which in principle all of the metal sites could be active sites. The enhanced reactivity of SACs and their unique reaction mechanisms originate from their unique structures and interactions with supports. The details of these structures are therefore the focus of intense investigation and debates. Among the factors hindering the progress in their investigation is the complexity of SAC systems, which is primarily related to the heterogeneity in their structures within the same sample. In this Account, we outline strategies that we have found to be useful for selected systems we have studied that can also be applied to many other SACs.

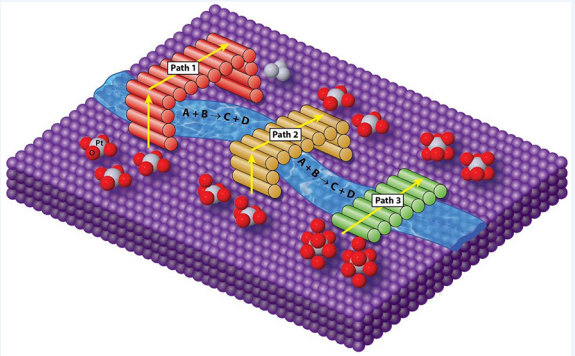

As an example of the most uniformly distributed SAC system, we focus on a Pt SAC support on nanoceria. A combination of imaging and spectroscopic techniques confirmed the atomic dispersion of Pt and the uniform distribution of Pt^{2+} single-atom sites. That uniformity was a prerequisite for determining the three-dimensional structure of Pt single atoms on the support surface. Our work illuminated the dependence of the structure and dynamics of Pt single atoms on the type of support. For Pt/ceria SACs, upon breaking of the Pt−O−Ce interaction at high temperatures under reductive conditions, the SACs aggregated into Pt nanoparticles that were active for the water gas shift reaction. In contrast, when Pt single atoms were anchored on the surface of a Co_3O_4 support, the removal of O in H_2 at high temperatures resulted in the formation of Pt_1Co_m/Co_3O_4 single-atom alloys (SAAs), which showed high N_2 selectivity for NO reduction. In SAAs with increased complexity, when the interparticle distribution of compositions of catalytically active species is narrow, advanced methods of X-ray absorption near-edge structure (XANES) analysis, e.g., those employing machine learning, allow their placements within "representative" particles to be deciphered and their changes in reaction conditions to be tracked.

Increasing the level of heterogeneity in the binding sites available to SACs blurs the resolution of spectroscopic methods such as X-ray absorption fine structure (XAFS) spectroscopy for detecting the details of their environments. We illustrate the effects of heterogeneity of the distribution of singly dispersed metal active sites using the PtNi/SBA-15 bimetallic catalyst as an example. In this system, the fact that Ni atoms existed in two types of species (the silicate phase and the PtNi nanoclusters) complicated the XAFS analysis, although when corrections for the silicate phase were applied, the results obtained from extended XAFS (EXAFS) data analysis helped to determine the three-dimensional structure of the PtNi nanoclusters.

While not a review of the field, this Account is aimed to share with the readers our efforts to resolve challenges due to many forms of structural complexity existing in most heterogeneous single-atom systems and obtain insights into the unique atomic structures, as inferred from the correlative use of multimodal characterization tools and advances in data analysis and modeling methods that we developed.

KEY REFERENCES

- Kottwitz, M.; Li, Y.; Palomino, R. M.; Liu, Z.; Wang, G.; Wu, Q.; Huang, J.; Timoshenko, J.; Senanayake, S. D.; Balasubramanian, M.; Lu, D.; Nuzzo, R. G.; Frenkel, A. I. Local Structure and Electronic State of Atomically Dispersed Pt Supported on Nanosized CeO_2. *ACS Catal.* **2019**, *9*, 8738−8748.[1] *This work determined the atomic*

Received: March 16, 2021
Published: May 14, 2021

https://doi.org/10.1021/acs.accounts.1c00180
Acc. Chem. Res. 2021, 54, 2660−2669

structure of Pt single atoms homogeneously dispersed on the surface of nanosized ceria. The isolated Pt^{2+} ions were located at the hollow sites of the (100) surface planes of the CeO_2 support, neighboring with four nearest oxygen atoms at 1.995 Å and 4 second-nearest Ce atoms at 3.34 Å.

- Nguyen, L.; Zhang, S.; Wang, L.; Li, Y.; Yoshida, H.; Patlolla, A.; Takeda, S.; Frenkel, A. I.; Tao, F. Reduction of Nitric Oxide with Hydrogen on Catalysts of Singly Dispersed Bimetallic Sites Pt_1Co_m and Pd_1Co_n. *ACS Catal.* **2016**, *6*, 840−850.[2] *This work studied the active species in 0.5 atom % Pt(Pd)/Co_3O_4 for reduction of NO with H_2. In these catalysts, Pt_1Co_n or Pd_1Co_m single-atom alloys were formed and found to be responsible for the high selectivity for N_2 production at elevated temperatures.*
- Marcella, N.; Liu, Y.; Timoshenko, J.; Guan, E.; Luneau, M.; Shirman, T.; Plonka, A. M.; van der Hoeven, J. E. S.; Aizenberg, J.; Friend, C. M.; Frenkel, A. I. Neural network assisted analysis of bimetallic nanocatalysts using X-ray absorption near-edge structure spectroscopy. *Phys. Chem. Chem. Phys.* **2020**, *22*, 18902−18910.[3] *In this work, a method based on the use of an artificial neural network was developed to extract the structural descriptors of atomic environments of type A and B atoms in A−B intermetallic nanoalloys from their X-ray absorption near-edge structure spectra.*
- Liu, D.; Li, Y.; Kottwitz, M.; Yan, B.; Yao, S.; Gamalski, A.; Grolimund, D.; Safonova, O. V.; Nachtegaal, M.; Chen, J. G.; Stach, E. A.; Nuzzo, R. G.; Frenkel, A. I. Identifying Dynamic Structural Changes of Active Sites in Pt−Ni Bimetallic Catalysts Using Multimodal Approaches. *ACS Catal.* **2018**, *8*, 4120−4131.[4] *This work revealed the structure complexity in the SBA-15 mesoporous silica-supported PtNi bimetallic nanoparticles. The metal−support reaction resulted in the formation of a nickel silicate phase at the interface that facilitated the formation of Pt−Ni heterometallic bonds on the surface of bimetallic nanoparticles. The surface heterometallic bonds were obtained to account for the improved selectivity for CO production during the reversed water gas shift reaction.*

1. INTRODUCTION

Single-atom catalysts (SACs), in which metal atoms are singly dispersed on supports, have attracted much attention in the past decade. In 2011, Zhang and co-workers described the reactivity of isolated Pt atoms anchored on FeO_x for CO oxidation and named this type of catalysts as single-atom catalysts.[5] In 2012, the work of Sykes and Flytzani-Stephanopoulos demonstrated a unique type of SAC: a single-atom alloy (SAA). It consisted of isolated Pd atoms in a Cu surface and was shown to be effective for selective heterogeneous hydrogenations.[6] Since then, numerous efforts have been focused on developing synthesis methods for preparing novel and stable SACs, exploring the applications of SACs in heterogeneous catalysis, understanding the working mechanisms of SACs, and characterizing the structure and structural dynamics of SACs under reaction conditions.[7−9] For all of those efforts, obtaining reliable descriptions of the electronic/atomic structure of single atoms on the support and their interaction with the support holds the key to their success. Single-atom systems are devoid of the interparticle and intraparticle heterogeneities that complicate investigations of nanoparticles.[10,11] However, another type of heterogeneity plagues research on SACs: the one arising from the coexistence of multiple single-atom sites. Liu et al.[12] revealed that there were four different FeN_x species (x = 4−6) in the atomically dispersed Fe−N−C catalyst that showed different activities for the selective oxidation of the C−H bond. Ren et al. found multiple Pt single-atom sites with different Pt−O coordination numbers and valence states on the surface of an Fe_2O_3 support.[13] The decrease in Pt−O coordination number/decrease in Pt oxidation state led to increases in hydrogenation activity.[13] For a system involving a broad distribution of single-atom sites, if the heterogeneity is overlooked, a wrong model will result from the analysis, one that emphasizes a "representative" environment of SACs.

The state of the art in characterizing SACs is the combination of high-spatial-resolution electron microscopy techniques and ensemble-averaged spectroscopic techniques.[5,14−24] X-ray absorption fine structure (XAFS) stands out as perhaps one of the most widely used methods for characterizing the local structure of single atoms. Because it is element-specific, its most common application was for examining whether metal ions are singly dispersed. On the basis of XAFS analysis, the detection (or lack of thereof) of a metal−metal (M−M) contribution manifests (or disproves) the existence of M_n ensembles. With extended XAFS (EXAFS) and the advent of quantitative methods for analysis of X-ray absorption near-edge structure (XANES), such as those utilizing machine learning techniques, one can now get quantitative structural information around single atoms. In this Account, using our key references, we demonstrate its use for detecting and quantifying atomic environments in atomically dispersed catalysts. We use examples where such environments range from relatively uniform to the least uniform.

2. RELATIVELY UNIFORM DISTRIBUTIONS

Metal ions that constitute SACs do not necessarily have identical local bonding environments. Variations of structural environments and electronic properties between sites result in variations of their catalytic properties.[25] The coexistence of multiple sites challenges current imaging and spectroscopy techniques and complicates the determination of the structural features and explanation of the catalytic mechanism of the best-performing site. Another challenge to most characterization techniques is the low weight loading of metal atoms in SACs. However, some SAC systems, e.g., single-site catalysts,[26] are more uniform than the others. Establishing the benchmark characterization capabilities and assembling a toolbox for SAC studies are important for understanding heterogeneous environments and the limitations to characterization that they present. We therefore open up the list of examples described in this Account with cases of SACs and SAAs where we were able to paint a detailed picture of their "representative" environment using their relatively high degree of uniformity.

2.1. Single-Atom Catalysts on Oxide Supports

To improve the weight loading of single atoms (Pt on ceria support), a nanosized ceria support was used in ref 1. Pt-doped $Ce(OH)CO_3$ nanoparticles were first produced on the surface of a commercial ceria support, which resulted in a uniform distribution of Pt single atoms after subsequent calcination. The Pt weight loading in the sample was 1.84%, which is relatively high for SACs. The size and distribution of Pt species

https://doi.org/10.1021/acs.accounts.1c00180
Acc. Chem. Res. 2021, 54, 2660−2669

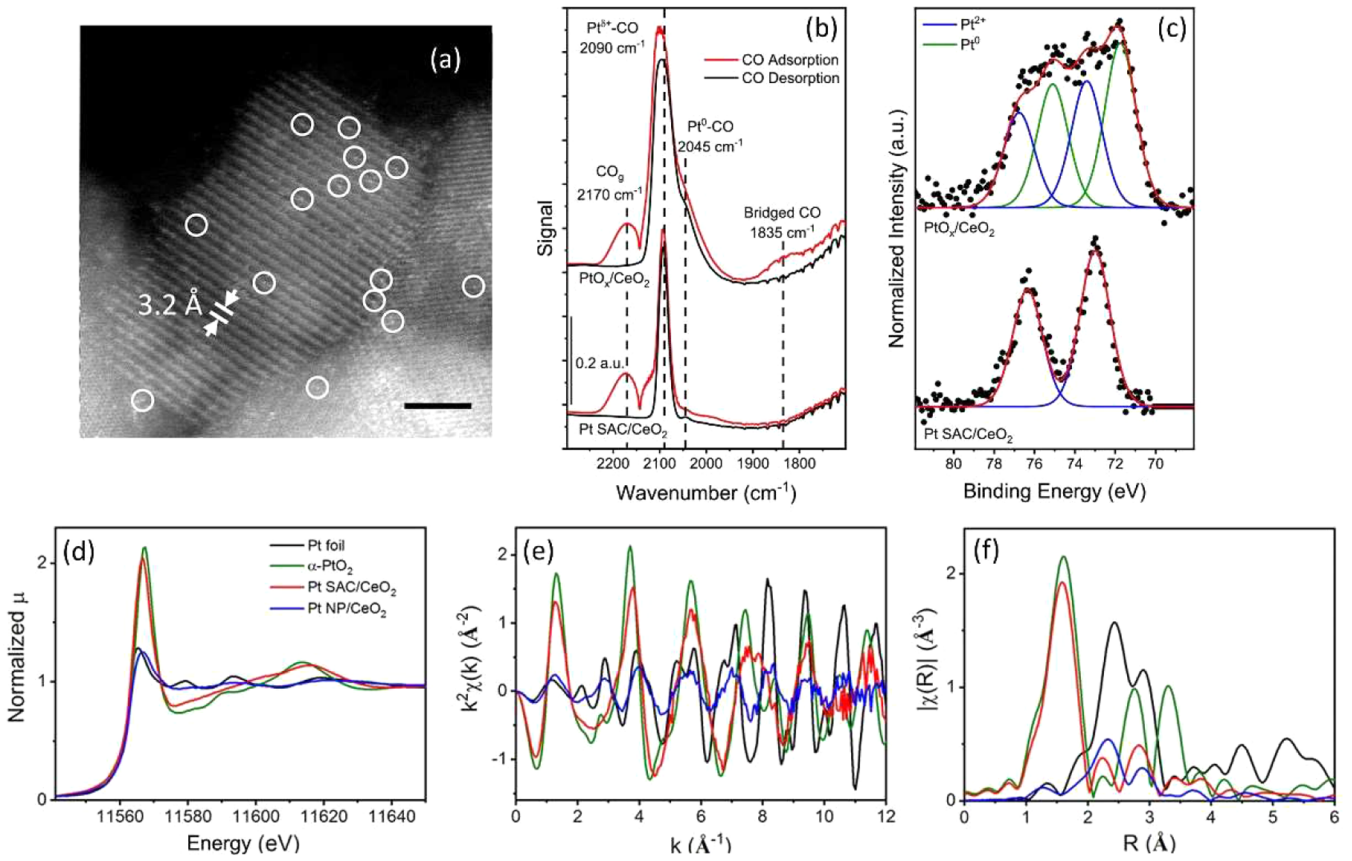

Figure 1. (a) STEM image of Pt/nanosized ceria. The scale bar is 2 nm. (b) DRIFTS spectra after CO adsorption (red) and CO desorption (black) on Pt/nanosized ceria. (c) Pt 4f XPS spectra for Pt/nanosized ceria samples with Pt^{2+} (blue) and Pt^0 (green) fitting curves. In (b) and (c), the spectra of PtO_x clusters on ceria are also included for comparison. (d–f) Pt L_3-edge XAFS spectra of Pt/nanosized ceria: (d) XANES; (e) EXAFS spectra in **k** space; and (f) EXAFS spectra in **R** space. For comparison, the XAFS spectra of standards (Pt foil and α-PtO_2) and reduced PtO_x/ceria are also included. Reproduced from ref 1. Copyright 2019 American Chemical Society.

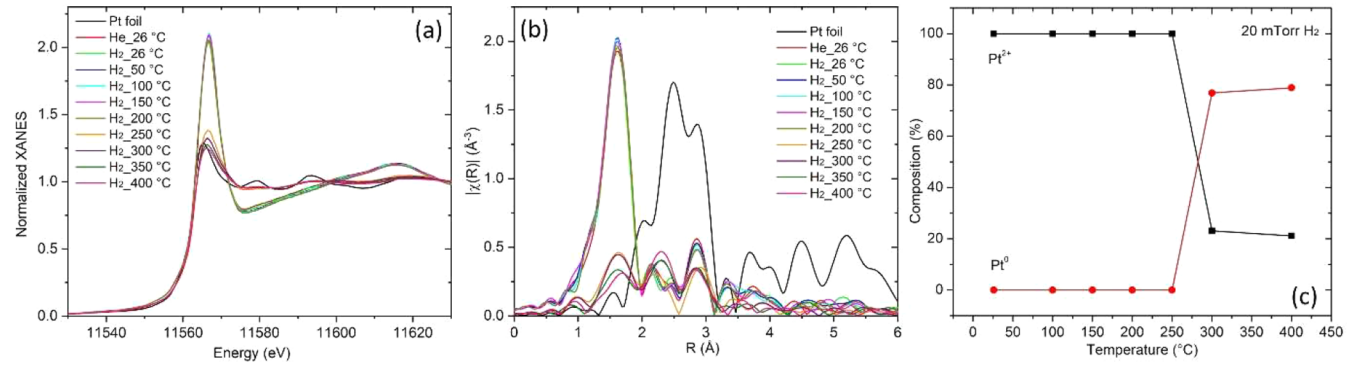

Figure 2. Temperature-dependent Pt L_3-edge (a) XANES and (b) EXAFS spectra of Pt/nanosized ceria under H_2 treatment. For comparison, the spectra of Pt foil are also included. (c) Temperature-dependent valence-state change of Pt in Pt/nanosized ceria under H_2 treatment.

were examined by scanning transmission electron microscopy (STEM), diffuse-reflectance infrared Fourier transform spectroscopy (DRIFTS), X-ray photoelectron spectroscopy (XPS), and XAFS (Figure 1). The STEM images of the as-prepared sample suggested that most likely Pt atoms were singly dispersed, and no nanoscale Pt species were observed. The position and shape of the CO band indicated that Pt single-atom species were the only species on the surface of ceria and that in these species Pt was in the 2+ state, as suggested by the XPS results. Unlike PtO_2 and nanoparticles, in these Pt single-atom species, Pt had a unique interaction with the ceria support, as indicated by the unique electronic features of the ceria support and Pt single atom (revealed by valence-band XPS and Pt 5d resonant inelastic X-ray scattering (RIXS)).

The Pt XANES spectrum (Figure 2a) showed a strong white-line peak, indicating that Pt was oxidized. The EXAFS spectrum (Figure 2b) showed unique features between 2 and 3 Å in **R** space compared with Pt metal and PtO_2, suggesting that the local structure of Pt single atoms was different compared with the bulk references. EXAFS analysis demonstrated that the Pt neighbors were four O atoms at about 1.995 Å and four Ce atoms at about 3.34 Å from the central Pt atom. The lack of

https://doi.org/10.1021/acs.accounts.1c00180
Acc. Chem. Res. 2021, 54, 2660–2669

detectable Pt−Pt bonds confirmed that Pt atoms were singly dispersed in the Pt/ceria sample. In addition, DFT calculations were used to model the details of the local structure of Pt on the support. In the structure that provided the best match to the combined experimental data, Pt single atoms were located at the hollow sites of the (100) surface of the nanosized ceria. As shown in Figure 2c, under H_2 conditions, the Pt^{2+} single-atom structure is stable below 250 °C. Above 250 °C, metallic Pt nanoparticles were formed.

The electronic structure and geometry of supported single atoms depend strongly on the type of support and its properties.[25,27−29] For Pt/TiO_2, the isolated Pt cations were bound to two excess O atoms, forming PtO_2 units.[25] This structure remained as single atoms in a cationic charge state through thermal treatments in oxidative (450 °C in O_2) and reductive (250 °C in H_2) pretreatments. Compared with the prereduced Pt nanocluster/TiO_2, the Pt single site showed higher reactivity for CO oxidation.[27] Upon addition of 1 wt % Ce to the TiO_2 support, Pt single atoms stabilized at the CeO_x−TiO_2 interface exhibited much higher activity for CO oxidation at 140 °C compared with the Pt/TiO_2 catalyst.[28] For a Cu_2O film-supported Pt system, the Pt single atoms existed in a neutral charge state and were active for CO oxidation (best performance at 72 °C).[24] For γ-Al_2O_3, the Pt single atoms were anchored to the coordinatively unsaturated pentacoordinate Al^{3+} (Al^{3+}_{penta}) centers on the (100) facets of the γ-Al_2O_3 surface ($Pt/Al^{3+}_{penta} = 1$).[29] For $Ti_{3-x}C_2T_y$ (T = O, OH, F) MXene with abundant Ti vacancies, Pt (between 0 and 2+) single atoms took the sites previously occupied by Ti and formed strong interactions with the $Ti_{3-x}C_2T_y$ support via metal−carbon bonds.[30] For supports with oxygen vacancies, M_1−□−M_2 (M_1 = single atom; □ = oxygen vacancy; M_2 = metal from the support) linkages were formed. In such sites, one cation preferred the adsorption of oxygen while another preferred a vacancy, resulting in two metastable states with and without oxygen occupancy, respectively. As a result, the oxygen/oxygen vacancy in these sites was highly active and exhibited enhanced activity in several redox reactions.[31]

We will next take a look at SAAs, a subset of SACs that pose additional challenges and offer new kinds of rewards.

2.2. Single-Atom Alloys

In the past decade, SAAs have been explored for many chemical reactions.[8] Generally, in SAA catalysts, a small amount of isolated metal atoms is dispersed in the surface layer of a metal host (Figure 3a). Reducing the size of the metal support could be a strategy for further tuning the electronic and chemical properites of SAAs (Figure 3b). On one side, alloy catalysts often have distinct electronic and chemical properties compared with their parent metals. On the other side, in SAAs, single atoms show the free-atom-like electronic structure.[32] This results in adsorption properties of SAAs different from those of nano/bulk-scale species but similar to those of molecular metal complexes, which as homogeneous catalysts exhibit exceptional product selectivities. SAA catalysts could thus potentially provide a way to circumvent scaling relationships, which describe linear relationships between adsorption energies of related chemical species on metal surfaces and are widely used to determine reactivity descriptors and predict optimal catalysts for certain chemical reactions in heterogeneous catalysis.[33−35]

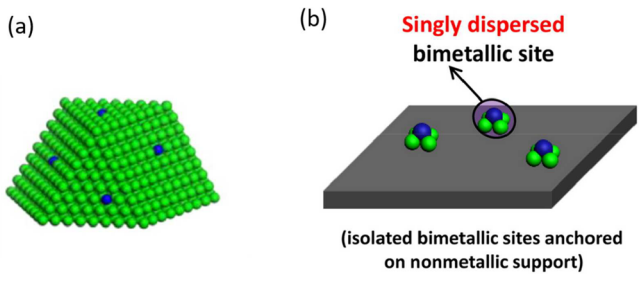

Figure 3. Schematics of single-atom alloys. (a) Single atoms (blue) anchored on a metal surface. (b) Singly dispersed bimetallic sites anchored on a nonmetallic support (gray). Reproduced from ref 2. Copyright 2015 American Chemical Society.

Oxide-supported single atoms can aggregate into nanoparticles but also transform into SAAs under the reaction conditions. The latter could be used to develop catalysts with novel structures and properties.[2,36] In the work described in ref 2, Nguyen et al. prepared Pt single atoms supported on Co_3O_4 nanorods. In the synthesis, Pt acetylacetonate was chosen since the steric effect of the large acetylacetonate group helps separate supported metal atoms. Low concentrations of the metal precursors were also used (0.1 and 0.5 atom %) to help avoid the aggregation of single atoms. The electron microscopy images (Figure 4a−d) demonstrated that the Pt atoms were singly dispersed. For the 0.5 atom % sample, about 48% of the Pt atoms were separated with a relatively short distance (0.5−1.5 nm) (Figure 4c,d). The Pt_1Co_m/Co_3O_4 catalyst was obtained by reducing the Pt/Co_3O_4 single-atom samples under 5% H_2 at 300 °C for 30 min. The treatment removed interfacial oxygen atoms and resulted in direct contact between Pt single atoms and Co from the support.

In the Pt_1Co_m/Co_3O_4 catalyst, Pt was in a cationic state, as indicated by Pt L_3-edge XANES (Figure 4e) and Pt 4d XPS (Figure 4f), suggesting that there was charge transfer between Pt and Co atoms. In the local atomic structure of the Pt_1Co_m/Co_3O_4 catalyst, Pt atoms neighbored with Co atoms, and no Pt−O or Pt−Pt bonds could be detected. The coordination number of Pt−Co was about 3.8, and the average bond distance was about 2.61 Å. The structure of the Pt_1Co_m/Co_3O_4 catalyst remained unchanged throughout the subsequent reaction conditions (NO + H_2 in the temperature regime of 25−300 °C) (Figure 4e,f), indicating that the Pt_1Co_m/Co_3O_4 catalyst was stable under the reaction conditions at elevated temperatures. In addition to the catalytic stability, the Pt_1Co_m/Co_3O_4 catalyst showed high activity and selectivity for NO reduction with H_2 ($2NO + 2H_2 \rightarrow N_2 + 2H_2O$). Specifically, starting from 150 °C, the NO conversion of the 0.5 atom % Pt_1Co_m/Co_3O_4 catalyst was almost 100%, and the selectivity for N_2 was 98% (Figure 4g,h). The 5 atom % Pt/Co_3O_4 catalyst also exhibited high NO conversion at 150 °C (and above), but the selectivity for N_2 was only about 60%, suggesting different intrinsic activities of the active sites in Pt_1Co_m/Co_3O_4 and those in Co_3O_4-suported Pt nanoparticles. The high selectivity of Pt_1Co_m/Co_3O_4 is mostly likely correlated with the Pt−Co sites, which facilitate the dissociation of NO and H_2.

2.3. Single-Atom Alloy Descriptors in Dilute Metal Alloys

In SAAs, structural characterization of catalytically active sites A (minority metal component) alloyed with B (majority metal component) has many similarities with other types of SACs. In all cases, the dilute regime, harsh reaction conditions, and structural changes of the catalysts in real time during the

https://doi.org/10.1021/acs.accounts.1c00180
Acc. Chem. Res. 2021, 54, 2660−2669

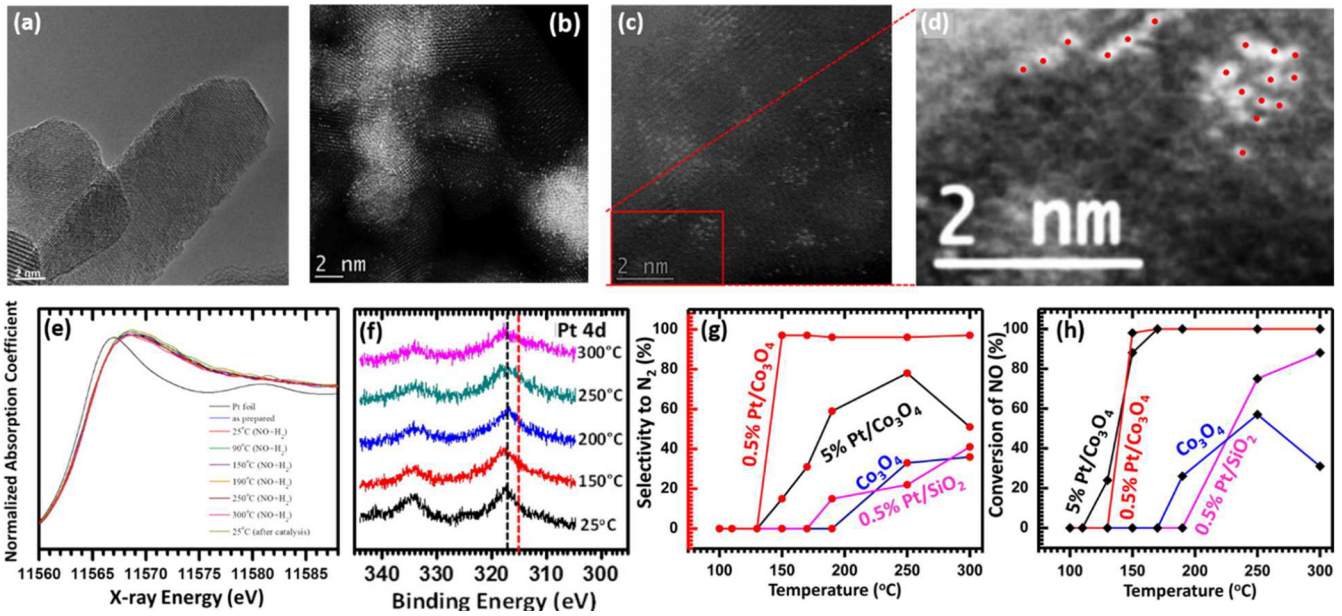

Figure 4. (a) High-resolution TEM image of Co_3O_4 nanorods. (b) Aberration-corrected high-angle annular dark-field scanning transmission electron microscopy (HAADF-STEM) image of 0.1 atom % Pt/Co_3O_4. (c, d) HAADF-STEM images of 0.5 atom % Pt/Co_3O_4. (e) Pt L_3-edge XANES of 0.5 atom % Pt/Co_3O_4 catalysts during catalysis in the mixture of reactant gases (NO + H_2) in the temperature regime of 25−300 °C after reduction in 5% H_2 for a half hour. (f) Pt 4d photoemission features of the as-synthesized 0.1 atom % Pt/Co_3O_4 after reduction at 300 °C in 5% H_2 for half an hour in a flow reactor integrated to AP-XPS. The pressure in the reactor during data acquisition was 1 Torr NO and 1 Torr H_2. (g, h) Comparison of catalytic selectivities (g) and activities (h) of 100 mg of 0.5 atom % Pt/Co_3O_4, 100 mg of 5 atom % Pt/Co_3O_4, 100 mg of pure Co_3O_4, and 100 mg of 0.5 atom % Pt/SiO_2 under the same catalytic conditions. Reproduced from ref 2. Copyright 2015 American Chemical Society.

reaction complicate their characterization by in situ/operando methods. As in the case of other SACs, SAAs are challenging for EXAFS analysis when bonding disorder is high because of, e.g., elevated temperatures or inherent strain, hence adversely affecting the signal-to-noise ratio in the EXAFS spectra. An alternative methodology that relies on XANES for quantitative determination of bimetallic architectures in dilute metal alloys in general, and SAAs in particular, was recently developed in the Frenkel group.[3] XANES features are more localized (in energy) and often quite intense compared with EXAFS features, and they are much less hampered by thermal disorder and low weight loading.

The neural-network-assisted data analysis of XANES spectra relies on the ability of theoretical spectroscopy codes to provide a large data set of labeled spectra, i.e., the pairs $\mu(E)-\{C_i\}$, where the absorption coefficient values (at the left) are the input and the structural descriptors of the catalyst (at the right) are the output. After being trained and validated, the artificial neural network (NN) can predict the descriptors of the catalyst on the basis of its XANES spectrum. The utility of this method was demonstrated on a series of Pd−Au bimetallic nanoalloys,[3] including ones with dilute Pd concentrations (2.6 atom % Pd in Au), thus relevant for SAA studies. Figure 5 presents the effects of gas and temperature treatment on component restructuring in the raspberry-colloid-templated (RCT) silica-supported 2.6 atom % Pd in Au catalyst. It shows in situ XANES data collected at room temperature under a He flow after calcination at 400 °C in 20% O_2/He balance and later, again at room temperature under He flow, after H_2 treatment at 400 °C. For that catalyst, EXAFS analysis at the Pd K edge is not sensitive to the Pd−Pd coordination number because the Pd−Pd contribution is dwarfed by the dominant Pd−Au contribution to EXAFS. XANES, however, shows an

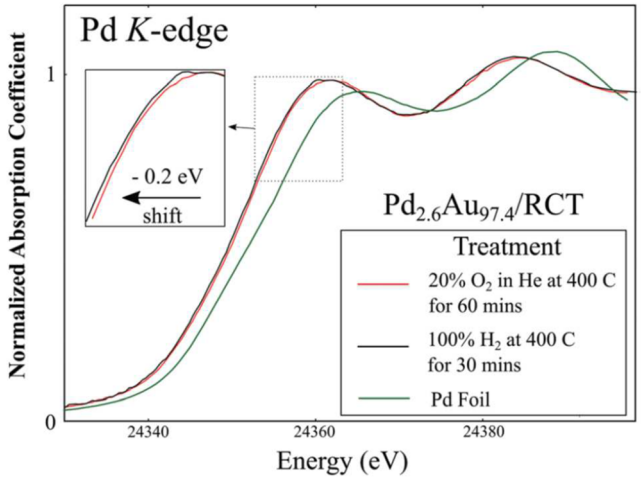

Figure 5. Pd K-edge XANES spectra of the $Pd_{2.6}Au_{97.4}$ catalyst after O_2 and H_2 treatments and bulk Pd reference foil. The XANES data were collected at room temperature under He. Reproduced with permission from ref 3. Copyright 2020 The PCCP Owner Societies.

interesting trend that can be qualitatively understood. Figure 5 shows that the local compositional motif around Pd atoms changes between different regimes. The data taken after H_2 treatment show a visible shift toward lower energy (i.e., away from Pd foil spectrum) and thus are consistent with a relatively larger degree of Pd alloying with Au compared with the data taken after O_2/He treatment.

For bimetallic materials, the information about the first-nearest-neighbor coordination numbers C_{AA} and C_{AB} (with respect to atom type A) and C_{BA} and C_{BB} (with respect to atom type B) is stored in the XANES spectra measured at the A and

https://doi.org/10.1021/acs.accounts.1c00180
Acc. Chem. Res. 2021, 54, 2660−2669

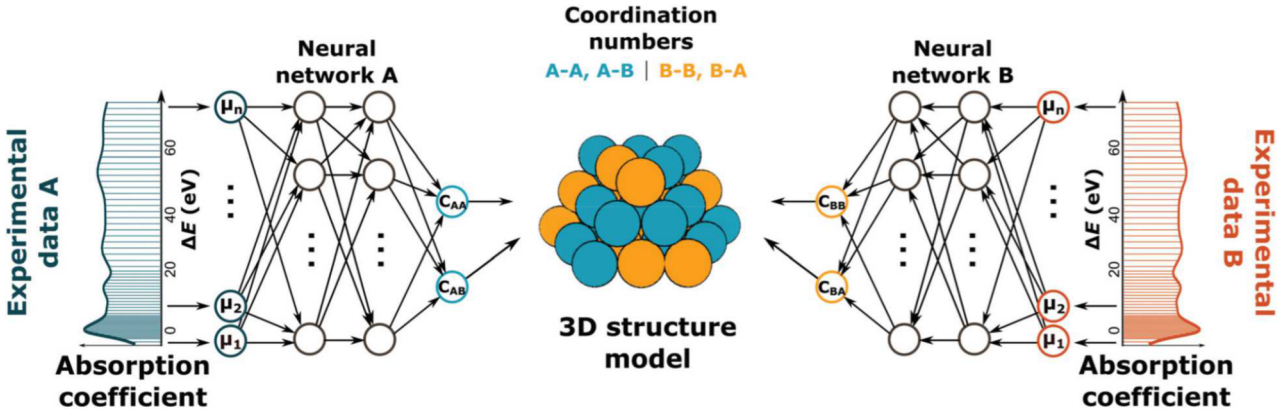

Figure 6. Schematic representing the application of NN-XANES to an A_xB_{1-x} bimetallic system. Partial first coordination numbers are extracted from the XANES of A and B absorbing components. The partial coordination numbers (A−A, A−B, B−B, and B−A) are used to deduce the locations of different alloy components within the alloy. For SAAs, the local structure around the dilute component (e.g., A) is particularly important, as it can be used to track its restructuring under the reaction conditions. Reproduced with permission from ref 3. Copyright 2020 The PCCP Owner Societies.

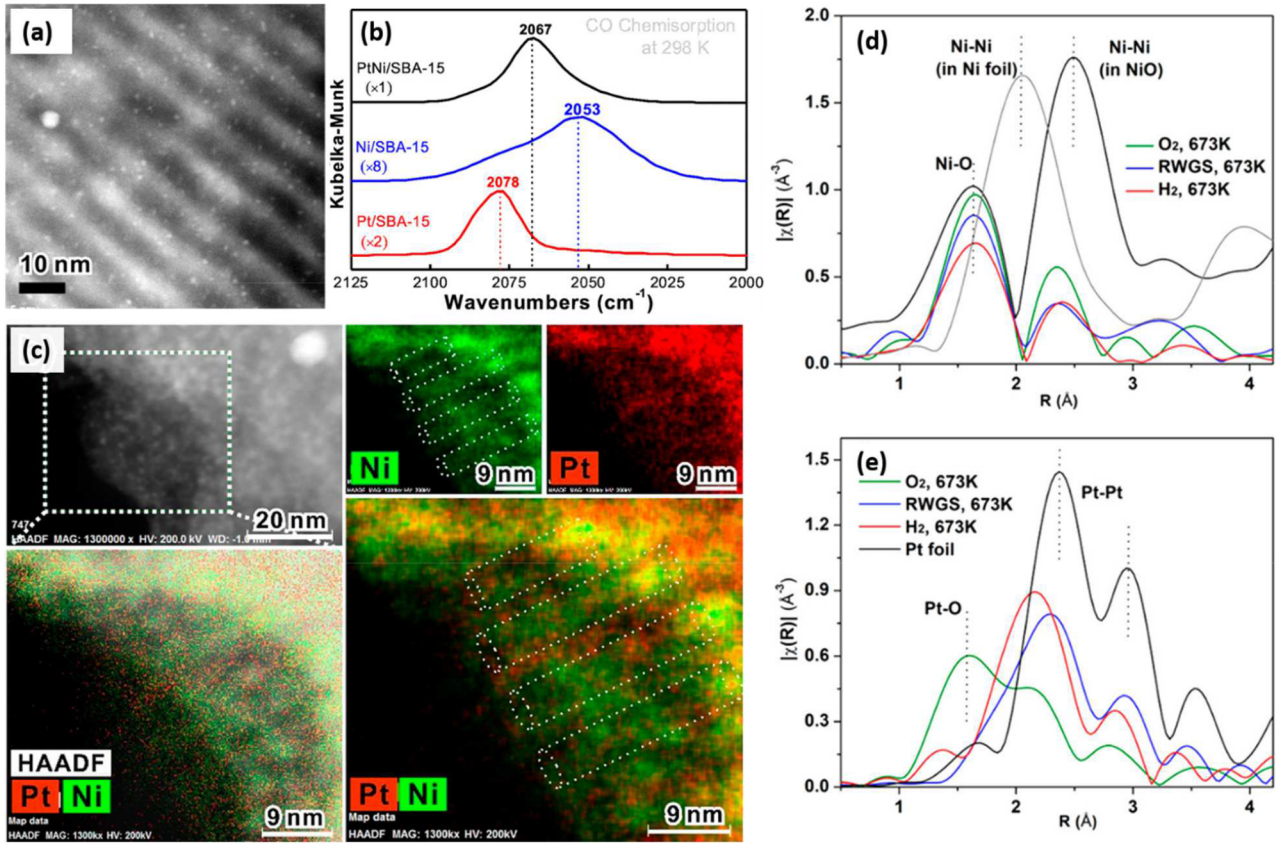

Figure 7. (a) Scanning transmission electron micrograph of the PtNi/SBA-15 catalyst. (b) DRIFTS band of CO atop adsorption on metallic sites of Ni, Pt, and PtNi catalysts (after activation in H_2 at 673 K) recorded at 298 K with a helium flow. (c) HAADF-STEM image and EDX maps showing the distributions of Ni and Pt in the PtNi/SBA-15 catalyst. (d) Ni K-edge and (e) Pt L_3-edge EXAFS spectra of PtNi/SBA-15 under the activation and reaction (reverse water gas shift) conditions. Reproduced from ref 4. Copyright 2018 American Chemical Society.

B absorption edges, respectively. To construct the NN for "inverting" the XANES spectrum and obtain the local coordination numbers, we adapted our previously developed NN-based methods[37,38] to the bimetallic materials. Briefly, the absorber-specific NNs (Figure 6) were constructed, each with pair-specific outputs. The NN was validated by both the theoretical data sets constructed using the FEFF9 code and experimental data with the known (from EXAFS) distribution of bimetallic components. More details about the construction of the neural network and its training, validation, and testing can be found in ref 3.

The NN-XANES method was shown to work for quantitative studies of gas and temperature treatment effects on component restructuring in the $Pd_{2.6}Au_{97.4}$ catalyst that we qualitatively discussed using raw data shown in Figure 5. The Pd−Pd coordination numbers extracted by the NN-XANES

https://doi.org/10.1021/acs.accounts.1c00180
Acc. Chem. Res. 2021, 54, 2660−2669

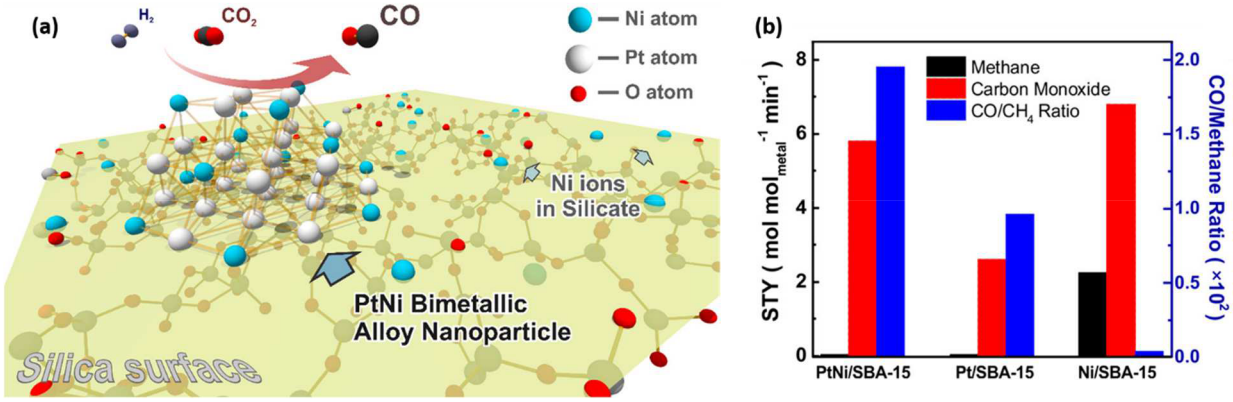

Figure 8. (a) Schematic model of a PtNi bimetallic nanoparticle on the silica surface with unreduced Ni ions in/on silicates. Platinum atoms are shown in gray and nickel atoms in teal. (b) Specific time yields (STYs) of CO and CH_4 over PtNi/SBA-15, Pt/SBA-15, and Ni/SBA-15 in the flow reactor test of the RWGS reaction at 673 K. All of the catalysts had the same molar loading of metals, and all of the specific time activities were normalized to that molar amount. Reproduced from ref 4. Copyright 2018 American Chemical Society.

method were found to decrease from 0.17 (obtained after the O_2/He treatment) to 0.10 (after the H_2 treatment), consistent with partial dissolution of Pd into the bulk.[3] Because the effect of H_2 affects all Pd atoms on the surface of all catalytic particles, the use of XAFS (and its analysis by NN-XANES) results in a reliable picture of the actual changes in the compositional motifs of *all* Pd–Au catalytic particles, not hampered by the ensemble averaging that affects less uniform systems, as described in greater detail below.

3. STRONGLY NONUNIFORM DISTRIBUTIONS

In SAA systems where the alloys have nanoscale dimensions, the strong interaction between the alloy components increases alloy stability but may also result in a heterogeneous distribution of metals within an alloy. To examine heterogeneity/homogeneity, in our studies of the mesoporous silica (SBA-15)-supported PtNi system, the particle size distribution was examined first. As shown in Figure 7a, the size distribution of supported nanoparticles was relatively narrow: 0.96 ± 0.22 nm. The position of the on-top CO band (measured by DRIFTS; Figure 7b) for the PtNi/SBA-15 sample suggested that the supported nanoparticle exposed a bimetallic surface.

For nanoscale bimetallic systems, except for the size distribution, a distribution of metal elements can be broad too, causing noticeable artifacts in EXAFS data analysis.[10,11] As suggested by energy-dispersive X-ray spectroscopy (EDX) maps (Figure 7c), there could be two types of distributions of Ni atoms: one type was colocalized with Pt atoms, and the other was on the surface of the support. The structure of the catalyst was studied by XAFS under different gas conditions (O_2, H_2 and reverse water gas shift (RWGS) reaction) at 400 °C (Figure 7d,e). On the basis of the EXAFS data analysis, under the H_2 and RWGS conditions, from the Pt perspective there were Pt–Ni and Pt–Pt paths, and the coordination number of Pt–Pt was larger, suggesting that Pt atoms formed a metallic cluster and that in the cluster Pt–Ni bimetallic bonds were in the minority. From the Ni perspective, there were Ni–O, Ni–Pt, and Ni–Si contributions. The existence of Ni–O and Ni–Si pairs suggested the strong interaction between Ni atoms and the silica support, while the absence of Ni–Ni bonds indicated that Ni atoms were singly dispersed in the Pt cluster.

With the obtained quantitative structural information, one could determine the atomic geometry of the PtNi nanocluster under the reaction conditions. Before this could be done, the coordination number of Ni–Pt had to be corrected since not all of the Ni atoms formed a heterometallic bond with Pt.[39] The correction should be derived from the mole fraction of Ni in the PtNi nanocluster. It was calculated by obtaining the mole fraction of Ni in the silicate phase using the measured Ni–Si coordination numbers.[4] The PtNi cluster size and the coordination numbers of Ni–Pt (corrected), Pt–Ni, and Pt–Pt were used as inputs for determining the atomic structure of the PtNi cluster. The schematic of the structure is shown in Figure 8a. It consisted of 37 atoms in total, generating an overall composition of $PtNi_{0.48}$ in the cluster. Ni atoms were singly dispersed on the surface without Ni–Ni bonding. This structure was stable under H_2 and RWGS conditions at 400 °C. Such stability could be correlated with the modified SBA-15 surface, in which some of the Ni atoms formed a nickel silicate with SBA-15. The heterogeneous distribution of Ni atoms also helped obtain the isolated distribution of Ni atoms on the surface of the Pt cluster, which resulted in the high activity and enhanced CO selectivity compared with SBA-15-supported Pt and Ni monometallic catalysts (Figure 8b). Alternatively, the γ-Al_2O_3-supported PtNi (singly dispersed Pt atoms) SAA facilitated the selective hydrogenation of CO_2 toward CH_4.[40]

In this PtNi/SBA-15 system, the silica support interacted with some of the Ni atoms and formed a nickel silicate phase.[4] In the Pt/Co_3O_4 catalyst described in the earlier section, the Pt atoms drew some Co atoms out of the Co_3O_4 support and formed Pt_1Co_m species.[2] In both cases, elements from the support were incorporated into the metal species. This phenomenon has recently attracted significant attention and is sometimes called a reactive metal–support interaction (RMSI).[41,42] Because of such interactions, in the Pt/Co_3O_4 catalyst, the resulting Pt_1Co_m species showed high activity and selectivity for the reaction of NO reduction.[2] In the PtNi/SBA-15 system, the nickel silicate phase helped improve the stability of ultrasmall PtNi single-atom alloys.[4] Similarly, Searles et al. grafted a platinum precursor onto the surface of silica-supported gallium single sites.[43] Subsequent reduction under H_2 at 500 °C led to the transformation of $Ga^{III}Pt^{II}/SiO_2$ to Ga_xPt ($0.5 < x < 0.9$; $Ga^{\delta+}$; Pt^0) bimetallic particles while a

https://doi.org/10.1021/acs.accounts.1c00180
Acc. Chem. Res. 2021, 54, 2660–2669

fraction of gallium remained as isolated surface sites on the support.[43] These isolated gallium surface sites provided Lewis acidic centers for particle stabilization in the reaction of propane dehydrogenation.[43] On the other hand, we want to note here that the heterogeneous distribution of metal elements imposes challenges onto many spectroscopic techniques. Complementary techniques should be combined, and data corrections should be applied, as demonstrated for the PtNi/SBA-15 system.[4]

4. CONCLUSION AND PERSPECTIVES

In this Account, we have highlighted the importance of recognizing the impact of heterogeneity of SACs on their properties and the challenges that multiple structures pose to characterization methods across different types of SACs, from singly dispersed metals on oxide supports to single-atom alloys. On one hand, singly dispersed atoms that constitute heterogeneous catalysts can exist in many different motifs, and that motivates the prospects of rational control of their surroundings and the design of catalysts with desired properties. For that, a prerequisite is the knowledge of the relationship between a possible structure of the catalytic active site and its function. If multiple structures coexist in the same system, several key questions should be addressed first: What are those structures that coexist in the catalytic system? Which ones show good activity, selectivity, and stability for a given product? Which ones are highly active but not stable? Which ones are highly stable but not active? Answering these questions requires that our characterization tools and analysis methods be able detect and quantify the heterogeneity that the SAC systems embed.

Another aspect that we attempted to cover, by highlighting examples from our work, is that catalytic systems may undergo restructuring under pretreatment and reaction conditions. For systems involving multiple metal sites, they will restructure differently, and some changes may be irreversible. For example, single sites that bind weakly with the support could aggregate into clusters/nanoparticles under the reaction conditions. Some changes could be environment-dependent and reversible. As a result, to discriminate between multiple sites and understand working mechanisms of SACs, combining multiple operando/in situ techniques with computational simulations is required.

AUTHOR INFORMATION

Corresponding Author

Anatoly I. Frenkel − *Department of Materials Science and Chemical Engineering, Stony Brook University, Stony Brook, New York 11794, United States; Division of Chemistry, Brookhaven National Laboratory, Upton, New York 11973, United States;* orcid.org/0000-0002-5451-1207; Email: anatoly.frenkel@stonybrook.edu

Author

Yuanyuan Li − *Department of Materials Science and Chemical Engineering, Stony Brook University, Stony Brook, New York 11794, United States;* orcid.org/0000-0003-3074-9672

Complete contact information is available at: https://pubs.acs.org/10.1021/acs.accounts.1c00180

Notes

The authors declare no competing financial interest.

Biographies

Yuanyuan Li received her Ph.D. degree from the University of Science and Technology of China. She is currently a research scientist working in Prof. Anatoly Frenkel's group in the Department of Materials Science and Chemical Engineering at Stony Brook University. Her research focuses on establishing structure−property relationships for rational design of catalysts.

Anatoly I. Frenkel is a Professor in the Department of Materials Science and Chemical Engineering at Stony Brook University and a Senior Chemist (joint appointment) at the Division of Chemistry of Brookhaven National Laboratory. He received his M.Sc. degree from St. Petersburg University and his Ph.D. degree from Tel Aviv University, all in Physics, followed by a postdoctoral appointment at the University of Washington. His research interests focus on the development and applications of in situ and operando synchrotron methods to solve a wide range of materials problems, with most recent emphasis on catalysis, electromechanical materials, filtration materials, and quantum dots, as well as machine learning methods for structural analysis and design of functional nanomaterials. He is a Fellow of the American Physical Society.

ACKNOWLEDGMENTS

The authors acknowledge support for the SAC studies summarized in this work by the U.S. Department of Energy (DOE), Office of Basic Energy Sciences, under Grant DE-FG02-03ER15476 and support for machine learning development of bimetallic nanocatalysts by the Integrated Mesoscale Architectures for Sustainable Catalysis (IMASC), an Energy Frontier Research Center funded by the U.S. DOE, Office of Science, Office of Basic Energy Sciences, under Award DE-SC9912573. Reaction tests and DRIFTS measurements at Brookhaven National Laboratory's Chemistry Division and XAFS data analysis were made possible through the Program Development Fund (21-017 to A.I.F.). We acknowledge multiple facilities where we performed our SAC work. The research described in this Account used beamlines 11-ID-C, 12-BM-B, and 20-ID-C of the Advanced Photon Source (APS), a U.S. DOE Office of Science User Facility operated for the DOE Office of Science by Argonne National Laboratory under Contract DE-AC02-06CH11357; beamline 8-ID of the National Synchrotron Light Source II, a U.S. DOE Office of Science User Facility operated for the DOE Office of Science by Brookhaven National Laboratory (BNL) under Contract DESC0012704; and beamline 2-2 of the Stanford Synchrotron Radiation Lightsource (SSRL), SLAC National Accelerator Laboratory, supported by the U.S. DOE, Office of Science, Office of Basic Energy Sciences, under Contract DE-AC02-76SF00515. We also used the microXAS beamline of the Swiss Light Source at the Paul Scherrer Institute (Villigen, Switzerland) and beamlines X18B and X19A of the National Synchrotron Light Source (NSLS), BNL. Operations at beamline 2-2 at SSRL and beamlines X18B and X19A at NSLS were supported in part by the Synchrotron Catalysis Consortium (U.S. DOE, Office of Basic Energy Sciences, Grant DE-SC0012335).

REFERENCES

(1) Kottwitz, M.; Li, Y.; Palomino, R. M.; Liu, Z.; Wang, G.; Wu, Q.; Huang, J.; Timoshenko, J.; Senanayake, S. D.; Balasubramanian, M.; Lu, D.; Nuzzo, R. G.; Frenkel, A. I. Local Structure and Electronic State of Atomically Dispersed Pt Supported on Nanosized CeO_2. *ACS Catal.* **2019**, *9*, 8738−8748.

(2) Nguyen, L.; Zhang, S.; Wang, L.; Li, Y.; Yoshida, H.; Patlolla, A.; Takeda, S.; Frenkel, A. I.; Tao, F. Reduction of Nitric Oxide with Hydrogen on Catalysts of Singly Dispersed Bimetallic Sites Pt_1Co_m and Pd_1Co_n. *ACS Catal.* **2016**, *6*, 840−850.
(3) Marcella, N.; Liu, Y.; Timoshenko, J.; Guan, E.; Luneau, M.; Shirman, T.; Plonka, A. M.; van der Hoeven, J. E. S.; Aizenberg, J.; Friend, C. M.; Frenkel, A. I. Neural Network Assisted Analysis of Bimetallic Nanocatalysts Using X-ray Absorption near Edge Structure Spectroscopy. *Phys. Chem. Chem. Phys.* **2020**, *22*, 18902−18910.
(4) Liu, D.; Li, Y.; Kottwitz, M.; Yan, B.; Yao, S.; Gamalski, A.; Grolimund, D.; Safonova, O. V.; Nachtegaal, M.; Chen, J. G.; Stach, E. A.; Nuzzo, R. G.; Frenkel, A. I. Identifying Dynamic Structural Changes of Active Sites in Pt−Ni Bimetallic Catalysts Using Multimodal Approaches. *ACS Catal.* **2018**, *8*, 4120−4131.
(5) Qiao, B.; Wang, A.; Yang, X.; Allard, L. F.; Jiang, Z.; Cui, Y.; Liu, J.; Li, J.; Zhang, T. Single-Atom Catalysis of Co Oxidation Using Pt_1/FeO_x. *Nat. Chem.* **2011**, *3*, 634−641.
(6) Kyriakou, G.; Boucher, M. B.; Jewell, A. D.; Lewis, E. A.; Lawton, T. J.; Baber, A. E.; Tierney, H. L.; Flytzani-Stephanopoulos, M.; Sykes, E. C. H. Isolated Metal Atom Geometries as a Strategy for Selective Heterogeneous Hydrogenations. *Science* **2012**, *335*, 1209−1212.
(7) Liu, Q.; Zhang, Z. Platinum Single-Atom Catalysts: A Comparative Review Towards Effective Characterization. *Catal. Sci. Technol.* **2019**, *9*, 4821−4834.
(8) Hannagan, R. T.; Giannakakis, G.; Flytzani-Stephanopoulos, M.; Sykes, E. C. H. Single-Atom Alloy Catalysis. *Chem. Rev.* **2020**, *120*, 12044−12088.
(9) Qin, R.; Liu, K.; Wu, Q.; Zheng, N. Surface Coordination Chemistry of Atomically Dispersed Metal Catalysts. *Chem. Rev.* **2020**, *120*, 11810−11899.
(10) Frenkel, A. I.; Wang, Q.; Sanchez, S. I.; Small, M. W.; Nuzzo, R. G. Short Range Order in Bimetallic Nanoalloys: An Extended X-ray Absorption Fine Structure Study. *J. Chem. Phys.* **2013**, *138*, 064202.
(11) Frenkel, A. I.; Yevick, A.; Cooper, C.; Vasic, R. Modeling the Structure and Composition of Nanoparticles by Extended X-ray Absorption Fine-Structure Spectroscopy. *Annu. Rev. Anal. Chem.* **2011**, *4*, 23−39.
(12) Liu, W.; Zhang, L.; Liu, X.; Liu, X.; Yang, X.; Miao, S.; Wang, W.; Wang, A.; Zhang, T. Discriminating Catalytically Active Fenx Species of Atomically Dispersed Fe−N−C Catalyst for Selective Oxidation of the C−H Bond. *J. Am. Chem. Soc.* **2017**, *139*, 10790−10798.
(13) Ren, Y.; Tang, Y.; Zhang, L.; Liu, X.; Li, L.; Miao, S.; Sheng Su, D.; Wang, A.; Li, J.; Zhang, T. Unraveling the Coordination Structure−Performance Relationship in Pt_1/Fe_2O_3 Single-Atom Catalyst. *Nat. Commun.* **2019**, *10*, 4500.
(14) Marcinkowski, M. D.; Darby, M. T.; Liu, J.; Wimble, J. M.; Lucci, F. R.; Lee, S.; Michaelides, A.; Flytzani-Stephanopoulos, M.; Stamatakis, M.; Sykes, E. C. H. Pt/Cu Single-Atom Alloys as Coke-Resistant Catalysts for Efficient C−H Activation. *Nat. Chem.* **2018**, *10*, 325−332.
(15) Wei, H.; Huang, K.; Wang, D.; Zhang, R.; Ge, B.; Ma, J.; Wen, B.; Zhang, S.; Li, Q.; Lei, M.; Zhang, C.; Irawan, J.; Liu, L.-M.; Wu, H. Iced Photochemical Reduction to Synthesize Atomically Dispersed Metals by Suppressing Nanocrystal Growth. *Nat. Commun.* **2017**, *8*, 1490.
(16) Nie, L.; Mei, D.; Xiong, H.; Peng, B.; Ren, Z.; Hernandez, X. I. P.; DeLaRiva, A.; Wang, M.; Engelhard, M. H.; Kovarik, L.; Datye, A. K.; Wang, Y. Activation of Surface Lattice Oxygen in Single-Atom Pt/CeO_2 for Low-Temperature Co Oxidation. *Science* **2017**, *358*, 1419−1423.
(17) Lin, L.; Zhou, W.; Gao, R.; Yao, S.; Zhang, X.; Xu, W.; Zheng, S.; Jiang, Z.; Yu, Q.; Li, Y.-W.; Shi, C.; Wen, X.-D.; Ma, D. Low-Temperature Hydrogen Production from Water and Methanol Using Pt/A-Moc Catalysts. *Nature* **2017**, *544*, 80−83.
(18) Lucci, F. R.; Liu, J.; Marcinkowski, M. D.; Yang, M.; Allard, L. F.; Flytzani-Stephanopoulos, M.; Sykes, E. C. H. Selective Hydrogenation of 1,3-Butadiene on Platinum−Copper Alloys at the Single-Atom Limit. *Nat. Commun.* **2015**, *6*, 8550.
(19) Wei, H.; Liu, X.; Wang, A.; Zhang, L.; Qiao, B.; Yang, X.; Huang, Y.; Miao, S.; Liu, J.; Zhang, T. Feox-Supported Platinum Single-Atom and Pseudo-Single-Atom Catalysts for Chemoselective Hydrogenation of Functionalized Nitroarenes. *Nat. Commun.* **2014**, *5*, 5634.
(20) Hülsey, M. J.; Zhang, B.; Ma, Z.; Asakura, H.; Do, D. A.; Chen, W.; Tanaka, T.; Zhang, P.; Wu, Z.; Yan, N. In Situ Spectroscopy-Guided Engineering of Rhodium Single-Atom Catalysts for Co Oxidation. *Nat. Commun.* **2019**, *10*, 1330.
(21) Bi, Q.; Yuan, X.; Lu, Y.; Wang, D.; Huang, J.; Si, R.; Sui, M.; Huang, F. One-Step High-Temperature-Synthesized Single-Atom Platinum Catalyst for Efficient Selective Hydrogenation. *Research* **2020**, *2020*, 9140841.
(22) Ding, K.; Gulec, A.; Johnson, A. M.; Schweitzer, N. M.; Stucky, G. D.; Marks, L. D.; Stair, P. C. Identification of Active Sites in Co Oxidation and Water-Gas Shift over Supported Pt Catalysts. *Science* **2015**, *350*, 189−192.
(23) Chen, Y.; Ji, S.; Sun, W.; Chen, W.; Dong, J.; Wen, J.; Zhang, J.; Li, Z.; Zheng, L.; Chen, C.; Peng, Q.; Wang, D.; Li, Y. Discovering Partially Charged Single-Atom Pt for Enhanced Anti-Markovnikov Alkene Hydrosilylation. *J. Am. Chem. Soc.* **2018**, *140*, 7407−7410.
(24) Therrien, A. J.; Hensley, A. J. R.; Marcinkowski, M. D.; Zhang, R.; Lucci, F. R.; Coughlin, B.; Schilling, A. C.; McEwen, J.-S.; Sykes, E. C. H. An Atomic-Scale View of Single-Site Pt Catalysis for Low-Temperature Co Oxidation. *Nat. Catal.* **2018**, *1*, 192−198.
(25) Thang, H. V.; Pacchioni, G.; DeRita, L.; Christopher, P. Nature of Stable Single Atom Pt Catalysts Dispersed on Anatase TiO_2. *J. Catal.* **2018**, *367*, 104−114.
(26) Zhang, Z.; Chen, Y.; Zhou, L.; Chen, C.; Han, Z.; Zhang, B.; Wu, Q.; Yang, L.; Du, L.; Bu, Y.; Wang, P.; Wang, X.; Yang, H.; Hu, Z. The Simplest Construction of Single-Site Catalysts by the Synergism of Micropore Trapping and Nitrogen Anchoring. *Nat. Commun.* **2019**, *10*, 1657.
(27) DeRita, L.; Dai, S.; Lopez-Zepeda, K.; Pham, N.; Graham, G. W.; Pan, X.; Christopher, P. Catalyst Architecture for Stable Single Atom Dispersion Enables Site-Specific Spectroscopic and Reactivity Measurements of Co Adsorbed to Pt Atoms, Oxidized Pt Clusters, and Metallic Pt Clusters on TiO_2. *J. Am. Chem. Soc.* **2017**, *139*, 14150−14165.
(28) Yoo, M.; Yu, Y.-S.; Ha, H.; Lee, S.; Choi, J.-S.; Oh, S.; Kang, E.; Choi, H.; An, H.; Lee, K.-S.; Park, J. Y.; Celestre, R.; Marcus, M. A.; Nowrouzi, K.; Taube, D.; Shapiro, D. A.; Jung, W.; Kim, C.; Kim, H. Y. A Tailored Oxide Interface Creates Dense Pt Single-Atom Catalysts with High Catalytic Activity. *Energy Environ. Sci.* **2020**, *13*, 1231−1239.
(29) Kwak, J. H.; Hu, J.; Mei, D.; Yi, C.-W.; Kim, D. H.; Peden, C. H. F.; Allard, L. F.; Szanyi, J. Coordinatively Unsaturated Al^{3+} Centers as Binding Sites for Active Catalyst Phases of Platinum on γ-Al_2O_3. *Science* **2009**, *325*, 1670−1673.
(30) Zhao, D.; Chen, Z.; Yang, W.; Liu, S.; Zhang, X.; Yu, Y.; Cheong, W.-C.; Zheng, L.; Ren, F.; Ying, G.; Cao, X.; Wang, D.; Peng, Q.; Wang, G.; Chen, C. Mxene (Ti_3C_2) Vacancy-Confined Single-Atom Catalyst for Efficient Functionalization of CO_2. *J. Am. Chem. Soc.* **2019**, *141*, 4086−4093.
(31) Yu, K.; Lou, L.-L.; Liu, S.; Zhou, W. Asymmetric Oxygen Vacancies: The Intrinsic Redox Active Sites in Metal Oxide Catalysts. *Adv. Sci.* **2020**, *7*, 1901970.
(32) Greiner, M. T.; Jones, T. E.; Beeg, S.; Zwiener, L.; Scherzer, M.; Girgsdies, F.; Piccinin, S.; Armbrüster, M.; Knop-Gericke, A.; Schlögl, R. Free-Atom-Like D States in Single-Atom Alloy Catalysts. *Nat. Chem.* **2018**, *10*, 1008−1015.
(33) Zhao, Z.-J.; Liu, S.; Zha, S.; Cheng, D.; Studt, F.; Henkelman, G.; Gong, J. Theory-Guided Design of Catalytic Materials Using Scaling Relationships and Reactivity Descriptors. *Nat. Rev. Mater.* **2019**, *4*, 792−804.

https://doi.org/10.1021/acs.accounts.1c00180
Acc. Chem. Res. 2021, 54, 2660−2669

(34) Khorshidi, A.; Violet, J.; Hashemi, J.; Peterson, A. A. How Strain Can Break the Scaling Relations of Catalysis. *Nat. Catal.* **2018**, *1*, 263−268.
(35) Thirumalai, H.; Kitchin, J. R. Investigating the Reactivity of Single Atom Alloys Using Density Functional Theory. *Top. Catal.* **2018**, *61*, 462−474.
(36) Zhang, S.; Nguyen, L.; Liang, J.-X.; Shan, J.; Liu, J.; Frenkel, A. I.; Patlolla, A.; Huang, W.; Li, J.; Tao, F. Catalysis on Singly Dispersed Bimetallic Sites. *Nat. Commun.* **2015**, *6*, 7938.
(37) Timoshenko, J.; Frenkel, A. I. "Inverting" X-ray Absorption Spectra of Catalysts by Machine Learning in Search for Activity Descriptors. *ACS Catal.* **2019**, *9*, 10192−10211.
(38) Timoshenko, J.; Lu, D.; Lin, Y.; Frenkel, A. I. Supervised Machine-Learning-Based Determination of Three-Dimensional Structure of Metallic Nanoparticles. *J. Phys. Chem. Lett.* **2017**, *8*, 5091−5098.
(39) Frenkel, A. Solving the 3d Structure of Metal Nanoparticles. *Z. Kristallogr. - Cryst. Mater.* **2007**, *222*, 605−611.
(40) Kikkawa, S.; Teramura, K.; Asakura, H.; Hosokawa, S.; Tanaka, T. Ni−Pt Alloy Nanoparticles with Isolated Pt Atoms and Their Cooperative Neighboring Ni Atoms for Selective Hydrogenation of CO_2 toward CH_4 Evolution: In Situ and Transient Fourier Transform Infrared Studies. *ACS Appl. Nano Mater.* **2020**, *3*, 9633−9644.
(41) Penner, S.; Armbrüster, M. Formation of Intermetallic Compounds by Reactive Metal−Support Interaction: A Frequently Encountered Phenomenon in Catalysis. *ChemCatChem* **2015**, *7*, 374−392.
(42) van Deelen, T. W.; Hernández Mejía, C.; de Jong, K. P. Control of Metal−Support Interactions in Heterogeneous Catalysts to Enhance Activity and Selectivity. *Nat. Catal.* **2019**, *2*, 955−970.
(43) Searles, K.; Chan, K. W.; Mendes Burak, J. A.; Zemlyanov, D.; Safonova, O.; Copéret, C. Highly Productive Propane Dehydrogenation Catalyst Using Silica-Supported Ga−Pt Nanoparticles Generated from Single-Sites. *J. Am. Chem. Soc.* **2018**, *140*, 11674−11679.

https://doi.org/10.1021/acs.accounts.1c00180
Acc. Chem. Res. 2021, 54, 2660−2669